

Local structures of liquid water studied by x-ray emission spectroscopyS. Kashtanov,¹ A. Augustsson,² Y. Luo,^{1,*} J.-H. Guo,^{3,†} C. S  the,² J.-E. Rubensson,² H. Siegbahn,² J. Nordgren,² and H.   gren¹¹*Theoretical Chemistry, Royal Institute of Technology, SCFAB, SE-10691, Stockholm, Sweden*²*Department of Physics, Uppsala University, SE-752 37 Uppsala, Sweden*³*Advanced Light Source, Lawrence Berkeley National Laboratory, Berkeley, California 94720, USA*

(Received 4 July 2003; published 9 January 2004)

The O $K\alpha$ x-ray emission spectra of water clusters with different sizes and conformations embedded in a continuum medium are simulated. The calculations have successfully explained the experimental spectra of water in both gas and liquid phases. It is shown that the x-ray emission spectra are very sensitive to the local hydrogen bonding structures. Strong electron sharing between different water molecules is observed and its possible connection to the covalency of hydrogen bonding is discussed. The experimentally observed strong excitation energy dependence of the spectra has been interpreted in terms of the polarization and angular dependence for the gas phase, and in terms of variations of local hydrogen bonding structures for the liquid phase.

DOI: 10.1103/PhysRevB.69.024201

PACS number(s): 78.70.En, 33.15.Fm, 79.90.+b, 82.90.+j

I. INTRODUCTION

The simplicity of the water molecule with its electron-poor nondegenerate electronic structure has made it an obvious test bed and demonstration case for spectroscopy as well as for theoretical modeling, something that in a certain sense contrasts the complexity of liquid water and the rather conspicuous difficulties of determining even the most basic properties of the solvated water molecule. The use of x-ray spectroscopy (not to be confused with x-ray diffraction scattering), has, however, not been used often in the context of liquid water, owing to some previous technical problems of sample handling in ultrahigh vacuum conditions. Thus only now, a quarter of a century after the first recording of soft x-ray emission (XES) of free water with molecular orbital resolution,¹ is a similar effort possible for the liquid case.² This time lag is somewhat unfortunate from the viewpoint of the inherent probing characteristics of x-ray spectroscopy for molecules and materials with element, positional and orientational specificity, and with local bond and building block probing capability, which have been extensively used in molecular and solid state studies, but which so far have not been fully carried over to the liquid phase. Furthermore, in comparison with commonly used electron based spectroscopies the deeply penetrating x-ray radiation truly probes bulk properties, thus avoiding surface structures with strong orientational correlation³ and even with icelike configurations, which will have special implications for the liquid shifts.^{3,4} The generalization and verification of the so-called final state rule to cover other systems than solids, have further increased the prospects of using soft x-ray emission as a general electronic structure probe.⁵

It was clearly demonstrated in our first study on x-ray emission of liquid water² that using current synchrotron radiation techniques it is indeed possible to obtain new information concerning both geometric and electronic structure. The chemical and physical features of liquid water are complicated and controlled by the presence of the strong hydrogen bonding. Many models were proposed to view the de-

tails of how liquid water is geometrically organized. There is at present a general consensus that liquid water is a macroscopic network of molecules connected by frequent and transient hydrogen bonds, which allow unbonded neighbors to occur in numbers that vary with temperature and pressure.⁶⁻¹² In contrast to the geometrical structure, information about the electronic structure of liquid water remains largely unknown due to the lack of proper experimental techniques. By comparing x-ray emission spectra of water in gas and liquid phases, the influence of the intermolecular interaction on the local electronic structure of liquid water has been directly observed,² revealing a strong electron sharing among water molecules. It was also shown that through resonant excitation, one particular three-hydrogen-bonding structure, where one hydrogen bond is broken, can be separately identified,² confirming the finding of the x-ray absorption study (XAS).¹³

Theoretical simulations have played an essential role in understanding the spectra. The complexity of the liquid systems has made it impossible to interpret the spectra with physical intuition alone. It is also a rather formidable task to treat the whole liquid system explicitly. The fact that x-ray spectroscopy probes mainly the local information has simplified the theoretical simulations drastically. A cluster model which contains a few solvation shells has been proven to be well adequate to describe both the absorption¹³ and the emission² spectra of liquid water. It was shown that XES spectra calculated by a simple semi-continuum model that consists of only the first solvation shell embedded in a continuum dielectric medium, captures all major features of the experimental results.² One main intention of the present paper is to provide details of theoretical models and simulations. We present experimental measurements of resonant XES of water in gas and liquid phases. The connection between spectral profiles and local hydrogen bonding structures is revealed. The origin of electron sharing among water molecules in the liquid phase has been given a special consideration.

II. COMPUTATIONAL DETAILS

The water molecule can act as both hydrogen donor and hydrogen acceptor, and can in principle form hydrogen bonds with four neighboring water molecules, being hydrogen donor for two of them and hydrogen acceptor for the other two, which is the case in cubic ice. However, in the liquid phase, the situation becomes complicated. Water molecules are constantly moving and can often be hydrogen bonded to less than four neighbors, forming so-called broken hydrogen bonding structures. We have chosen three representative clusters from those used in previous simulations for XAS (Ref. 13) and XES (Ref. 2) of liquid water. They cover three solvation shells and contain 26 to 28 water molecules with different local hydrogen bonding structure already in the first solvation shell. One of them has the typical four hydrogen bonding structure with tetrahedral coordination similar to that in ice, denoted as SYM. The other two clusters have broken asymmetrical hydrogen bonding structure. They can be further distinguished from the local position of the broken hydrogen bond: either a missing bond at the hydrogen site (A-ASYM) or at the oxygen site (D-ASYM). We have used the same notations as proposed in Ref. 13. The coordinations of these clusters are taken out from molecular dynamics (MD) simulations of Ojamäe.^{13,16} The use of molecular dynamics allows us to have realistic structures to work with. However, it should be mentioned that the interpretation of x-ray emission spectra does not depend so much on the quality of the MD methods applied.

Full geometry optimization of the single water molecule was performed at the Hartree-Fock level with Sadlej basis set¹⁴ using the DALTON program.¹⁵ The choice of this basis is based on long experience. Nonresonant and resonant x-ray emission spectra of all clusters were also calculated at the same level and the same basis set. We have taken into account the long-range intermolecular interactions by embedding the clusters into a dielectric medium, for which a multipole reaction field theory is applied. A spherical cavity is adopted and with a radius equal to the molecular size plus the van der Waals radius of the outermost atoms. The group theory formulation developed by Luo *et al.*^{17,18} was used to calculate resonant XES. A Lorentzian function with line width of 0.5 eV is used to convolute the calculated spectra, which are shifted downward by 20 eV to compensate the core-hole effect. It should be noted that the vibrational motions are not treated in the present study.

III. EXPERIMENT

The experiments were performed at beamline 7.0.1 at the Advanced Light Source (ALS), Lawrence Berkeley National Laboratory. The beamline comprises a 99-pole, 5 cm period undulator and a spherical-grating monochromator covering the spectral energy range between 60–1300 eV.¹⁹ The incident photon beam entered a gas cell through a 1000 Å thick silicon nitride window. A gas pressure of a few mbar was maintained in the gas cell. As an exit window for the emitted x-rays a 1500 Å thick polyimide window was used. XAS spectra were obtained in the transmission detection mode.

The liquid samples were sealed in a cell in the liquid

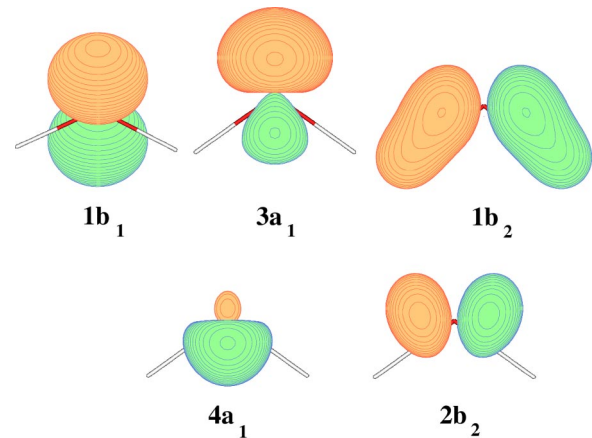


FIG. 1. Density pictures of three highest occupied orbitals $1b_2$, $3a_1$, and $1b_1$ and two lowest unoccupied orbitals $4a_1$ and $2b_2$ of the water molecule.

phase XAS and XES measurements. The incident photon beam entered and exited from the same silicon nitride window of 1000 Å thickness. XAS spectra of liquid water were measured by using the x-ray fluorescence-yield (FY) mode.

The resolution of the monochromator was set to 0.2 eV for the O $1s$ absorption edges. The XAS spectra were normalized by means of the photocurrent from a clean gold mesh in front of the sample to correct for intensity fluctuations in the photon beam. XES spectra were recorded using a high-resolution grating spectrometer.²⁰ The spectrometer was mounted parallel to the polarization vector of the incident photon beam, with its entrance slit oriented parallel to the direction of the incident beam. The length of the gas cell exit window allowed a large portion of the interaction region to be observed by the spectrometer. The resolution of the monochromator and spectrometer in the gas-phase measurements was approximately 0.65 and 1.0 eV, respectively. The resolution of the monochromator and spectrometer in liquid-phase measurements was approximately 0.45 and 0.5 eV, respectively.

IV. WATER MOLECULE

The water molecule belongs to the C_{2v} symmetry group with a ground state electronic configuration: $1a_1^2 2a_1^2 1b_2^2 3a_1^2 1b_1^2$. For x-ray emission spectroscopy water serves as an illustrative case for spectral resolution and for the useful feature of local probing of molecular orbitals: The outermost $1b_1$ lone-pair orbital receives maximum intensity in the local decomposition model, since this orbital has $2p$ character and is centered at the site of the core $1s$ orbital. From similar arguing the bonding, respectively, antibonding $3a_1$ and $1b_2$ orbitals are less intensive since they in addition to $O2p$ character also contain amplitudes on the hydrogens atoms. The deepest valence orbital, the $2a_1$ orbital with $O2s$ character, lacks intensity although, like the $1b_1$ orbital, it is centered on the oxygen, thus demonstrating that atomic dipole selection rules are operating even when having a lower molecular symmetry. Those three $2p$ -derived valence orbitals $1b_1$, $3a_1$, and $1b_2$ are shown in Fig. 1,

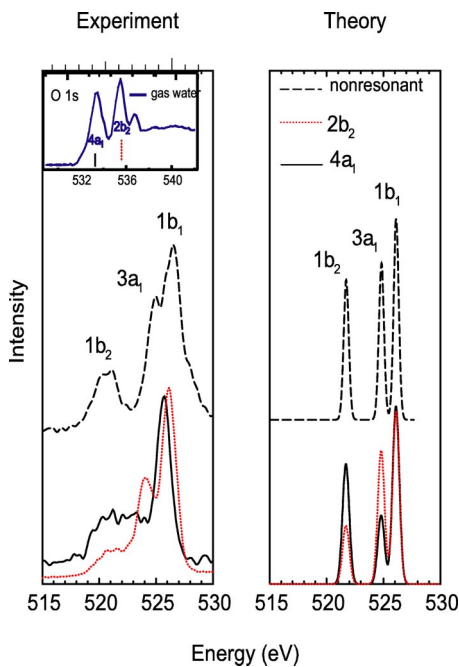


FIG. 2. Experimental and theoretical resonant and nonresonant emission spectra of water molecule in gas phase. The resonant emission spectra are generated from the resonant excitation to the $4a_1$ (in solid line) and $2b_2$ (in dotted line), respectively. The x-ray absorption spectrum is shown in the inset.

which have different orientations: $1b_2$ and $3a_1$ are lying in the molecular plane, whereas the lone pair orbital $1b_1$ is perpendicular to that plane.

Nonresonant XES of the gas phase water molecule is presented in Fig. 2, where the three outermost valence orbitals are clearly resolved. Their intensity distribution fits well with the orbital description given above. Remarkably, the same spectrum recorded by the same laboratory 25 years ago using a 3 m grazing incidence grating spectrometer¹ actually had slightly better resolution. The Hartree-Fock result of nonresonant XES shown in Fig. 2 is also in close agreement with previous theoretical results.²¹⁻²³ It is noted that calculations give quite good description for the spectral bands of $1b_1$ and $3a_1$, but not $1b_2$, with respect to the experiment in terms of both intensity profile and energy position. The $1b_2$ band of the experimental spectrum is much broader and is redshifted by 1 eV. Such differences have been established as due to the so-called lifetime-vibrational interference effect, which is a result of the short lifetime of the intermediate core hole state.²⁴ A full description of the lifetime-vibrational interference effect requires extensive computational efforts as shown in Ref. 24, which is difficult to apply for the larger system, such as the water clusters. We will though not take into account the vibrational contributions to the XES spectra in the present study. Similar difference between theory and experiment can be found for the case of liquid water, indicating a similar effect of lifetime-vibrational interference. It is obvious that without treating the vibrational motions, we will not be able to describe the proton transfer in liquid water.

The near-edge x-ray absorption spectrum of gas phase water shows two distinct features prior to the continuum, see

the inset of Fig. 2. They can be assigned to the lowest unoccupied orbital (LUMO) $4a_1$ and the second unoccupied orbital $2b_2$ (the orbital pictures of water can be found in Fig. 1). In Fig. 2, the resonant x-ray emission spectra of water are also shown. Clearly, the x-ray emission spectra are strongly dependent on the excitation energies. In comparison with the nonresonant case, resonant excitation to the LUMO ($4a_1$) level results in a 0.9 eV redshifting of orbital $1b_1$ and a noticeable intensity reduction for orbital $3a_1$. The observed redshifting is due to the screening effect that is enforced by the presence of an extra electron in the LUMO. The most significant difference caused by the excitation to $2b_2$ seems to be the decrease of intensity for $1b_2$. Such intensity changes can be rationalized by the polarization or angular dependence of the resonant x-ray emission.

It is possible to derive explicit formulas for the angular dependence of the X-ray emission from scattering theory applied to randomly oriented samples.¹⁸ The intensities can be expressed as

$$I(\theta) = I_{\perp}(\theta) + I_{\parallel}(\theta),$$

$$I_{\perp}(\theta) = \frac{1}{2} I_0 [1 - R],$$

$$I_{\parallel}(\theta) = \frac{1}{2} I_0 [1 + R(3 \sin^2 \theta - 1)], \quad (1)$$

where θ is the angle between the polarization vector of the incident photon and the propagation direction of the outgoing photon. I_0 is proportional to the total intensity emitted in all directions and summed over all polarization vectors and R is the polarization anisotropy parameter. The plane which defines \perp and \parallel is here defined as perpendicular to the direction of the incident radiation. With a spectrometer which is not polarization selective it is not possible to measure directly I_{\perp} or I_{\parallel} , but it is possible to measure the total intensity, $I(\theta)$, as a function of emission angle θ . The general expressions for the anisotropy parameter R and the intensity I_0 have been evaluated and a simple expression for the anisotropy parameters R was given in Ref. 18.

When the different final states are well separated, R has a rather simple expression for a particular state f :

$$R_f = \frac{1}{5} (3 \cos^2 \phi_f - 1), \quad (2)$$

where ϕ_f is an angle between the transition dipole moments of absorption and emission processes. For the case of water, when the excitation is to the LUMO $4a_1$, it gives

$$R_{a_1} = \frac{2}{5}, \quad R_{b_1, b_2, a_2} = -\frac{1}{5}. \quad (3)$$

For the excitation to the LUMO+1, $2b_2$, one has

$$R_{b_2} = \frac{2}{5}, \quad R_{a_1, b_1, a_2} = -\frac{1}{5}. \quad (4)$$

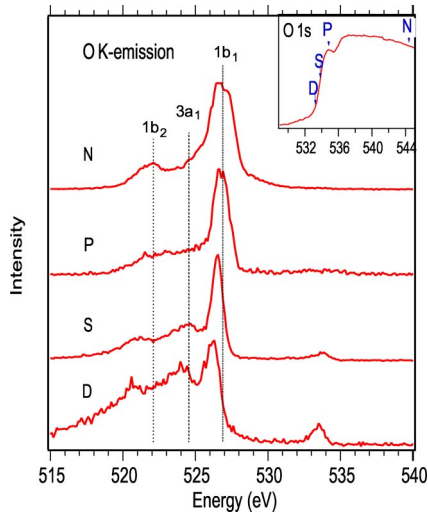


FIG. 3. Resonant x-ray emission spectra of liquid water. The arrows shown on the x-ray absorption spectrum (inset) indicate the excitation photon energies used.

The experimental spectra of water were detected at $\theta=0$, therefore, the emission intensity can be written as

$$I(0^0) = I_0(1 - R), \quad (5)$$

where I_0 can be referred to the nonresonant emission spectrum. One can thus expect that for excitation to $4a_1$ the emission intensity for a_1 orbitals should decrease, while for excitations to $2b_2$, the emission intensity of the b_2 orbital is reduced. This provides a perfect explanation for the experimental spectra of water and is indeed the picture obtained from the simulations, see Fig. 2.

V. LIQUID WATER

Recently, we reported experimental measurements and theoretical analysis of resonant x-ray emission of liquid water,² revealing detailed information about the electronic and local hydrogen bonding structures. We will recapture some of the important conclusions drawn from the previous study, and present a set of resonant x-ray emission spectra of liquid water and their connections to the local hydrogen bonding structures through theoretical simulations.

Upon liquefaction, the sharp spectral features in the XAS of gas phase water are turned into a broad band with a distinct preedge structure, see inset of Fig. 3. Such changes are caused by strong hydrogen bonding interactions and thermodynamic motions of water molecules. In particular, the preedge structure in the XAS of liquid water is attributed from one particular broken hydrogen bonding structure (D-ASYM) showed on Fig. 4, where one hydrogen bond is missing at the hydrogen donor site of the water.¹³ The resonant x-ray emission spectra of liquid water excited at energies *N* and *P* shown in Fig. 3 are the same as the ones presented in our previous work.² By comparing with the gas phase nonresonant spectrum, one can realize that the major change upon solvation is the intensity loss at the region corresponding to the bonding orbital $3a_1$ of the water molecule,

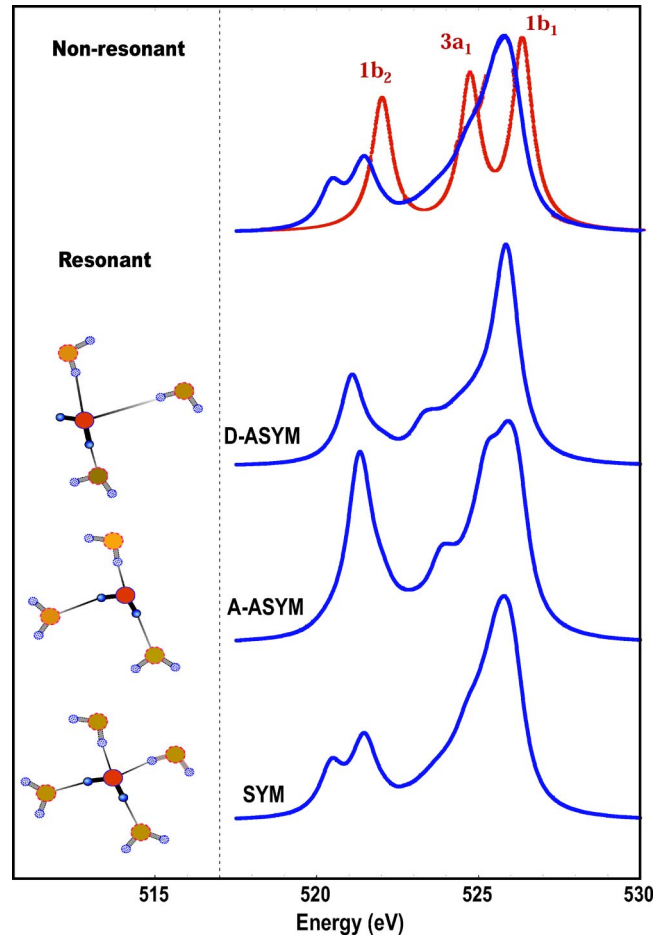


FIG. 4. Calculated nonresonant and resonant x-ray emission spectra of liquid water. The calculated nonresonant x-ray emission spectrum of gas phase water is added (thin line, sharp structure) for comparison.

which can be seen as the result of a strong molecular orbital mixing among different water molecules.² Similar changes at the $3a_1$ band upon solidification were observed in the photoelectron²⁵ and x-ray emission spectra of ice.²⁶ We have also found that the resonant spectrum of liquid water excited on top of the preedge shoulder is entirely due to the D-ASYM configuration, confirming the observation of the XAS study.¹³ All these findings are supported by the theoretical simulations as shown in Fig. 4. It should be mentioned that the major differences among three structures SYM, D-ASYM, and A-ASYM, is within the vicinity of the first solvation shell. It is quite remarkable that XES can be so sensitive to the local structures. We will present more striking cases in the discussion to follow.

Apparently, one can expect more local structures than those three discussed above to be present in liquid water. Molecular dynamic simulations have identified the existence of a small portion of structures with two or three broken hydrogen bonds.⁸ It was mentioned in Ref. 13 that the structure with only one donor and one acceptor generates an x-ray absorption spectrum similar to those obtained from D-ASYM. Therefore, it is impossible to distinguish its existence using x-ray absorption. In contrast, the selectivity of

the XES technique can provide the answer. We have measured two x-ray emission spectra excited at the lower energy side of the preedge shoulder with excitation energies 533.7 (S) and 533.2 eV (D), respectively. As can be seen from Fig. 3, spectrum S resembles spectrum P well, indicating that both are generated from similar structures. However, significant difference between spectrum D and the other two resonant spectra appears. Obviously, this spectrum receives contributions from a local structure that drastically differs from the D-ASYM. Calculations show that the most probable structures are those with two broken hydrogen bonds. The detailed discussion about the simulations will be presented in the next sections. In spectrum D one can see that the intensity at the $3a_1$ region increases greatly. The relative intensity of the two spectral bands $3a_1$ and $1b_1$ seems to be close to that for the gas phase. It is also noticed that both $3a_1$ and $1b_2$ bands are rather broad, implying that strong electron sharing also exists in this structure.

A. First solvation shell

We have shown in our previous report² that the first solvation shell with complete hydrogen bonds can reveal the most important features of the full spectra from either calculations of large clusters or from experiment. From now, we will concentrate on the spectral properties of different local first solvation structures, which are taken out from the big ASYM cluster. These clusters will be named after the number of donors and acceptor involved. For instance, a full hydrogen bonding system is simply labeled as *W-DDAA*, where *W* refers to the center water molecule we are interested in, *D* and *A* are the donor and the acceptor, respectively. The small clusters are taken out from the big ASYM cluster.

It is known that x-ray emission of a single molecule can be well described by the *p* population of the excited atom simply because of the local dipole selection rule. We have also examined this simple approach for the water clusters. Figure 5 displays the spectra of oxygen in a four hydrogen bonding structure *W-DDAA* calculated from both *p* population and full transition moments. The *p* orbitals involved in the *p* population analysis are the ones located on the center water molecule that is excited. Clearly, the *p*-population analysis works very well for the hydrogen bonded systems as well. Again, the strong electron sharing/orbital mixing between water molecules are observed in the *p*-population representation.

We prefer to interpret such electron sharing as a sign of covalency of hydrogen bonding as proposed by Pauling.²⁷ Isaacs *et al.*²⁸ claimed to have direct experimental evidence for a substantial covalent nature of the hydrogen bond based on the observation of periodic intensity variations in their Compton scattering measurements. However, their explanation was dismissed by theoretical calculations of Ghanty *et al.*,²⁹ who have shown that a calculation for the water dimer could reproduce the Compton scattering profile of Isaacs *et al.*, but failed to identify covalency in the bond between two water molecules. A recent periodic Hartree-Fock study on ice shows substantial charge transfer among

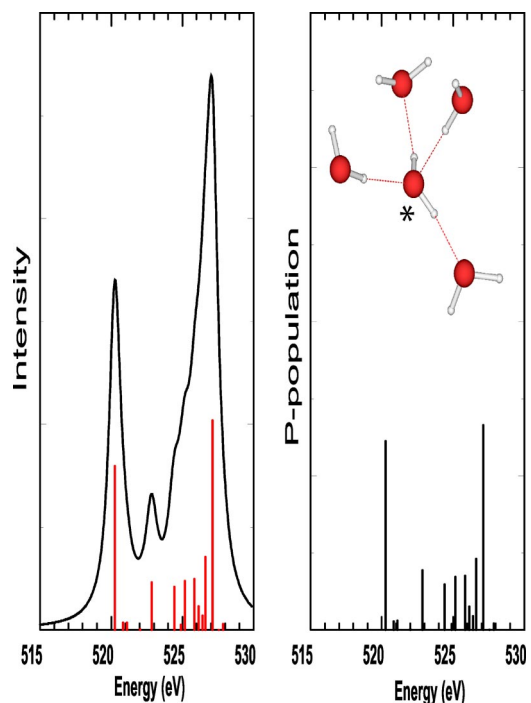


FIG. 5. X-ray emission spectra obtained from full transition moment calculations (left) and *p*-population analysis (right) for the first solvation shell structure with complete hydrogen bonds *W-DDAA*. The excited oxygen is marked with an asterisk.

water molecules in ice, indicating that the interaction between water molecules in ice is different from the gas phase.³⁰ It would thus be interesting to see what the x-ray emission spectrum of the water dimer can tell.

B. Water dimers

We first calculate spectra of the water dimer in gas phase using the geometry optimized by Klopper³¹ at the CCSD(T) level, giving an O-O distance R_{OO} between the two water molecules of 2.98 Å. With this configuration the spectra for the donor and acceptor molecules are quite similar, resembling the spectrum of single water, see Fig. 6. It should be noted that almost identical spectra have been obtained for the water dimer at the Hartree-Fock optimized geometry. The relative shifting between these two spectra can be easily understood in terms of a pure electrostatic interaction, which shows a typical push-pull behavior. We have also computed the spectra of an icelike dimer based on the geometry given by Ghanty *et al.*,²⁹ in this case the O-O distance is 2.75 Å. The spectra are almost the same as those obtained for the gas phase water dimer, but showing larger relative shifting and a small degree of orbital mixing. However, to a large extent, the electron sharing between water molecules in these two cases is small. The interaction between them is dominated by the pure electrostatic interaction. Ghanty *et al.*²⁹ showed that the periodic intensity variation in the Compton scattering measurements of Isaacs *et al.*²⁸ could be reproduced in the icelike water dimer with either Hartree-Fock or Kohn-Sham calculations. Therefore, the evidence provided by the Compton scattering experiment for ice cannot be viewed as a definite sign of covalency in hydrogen bonds of liquid water.

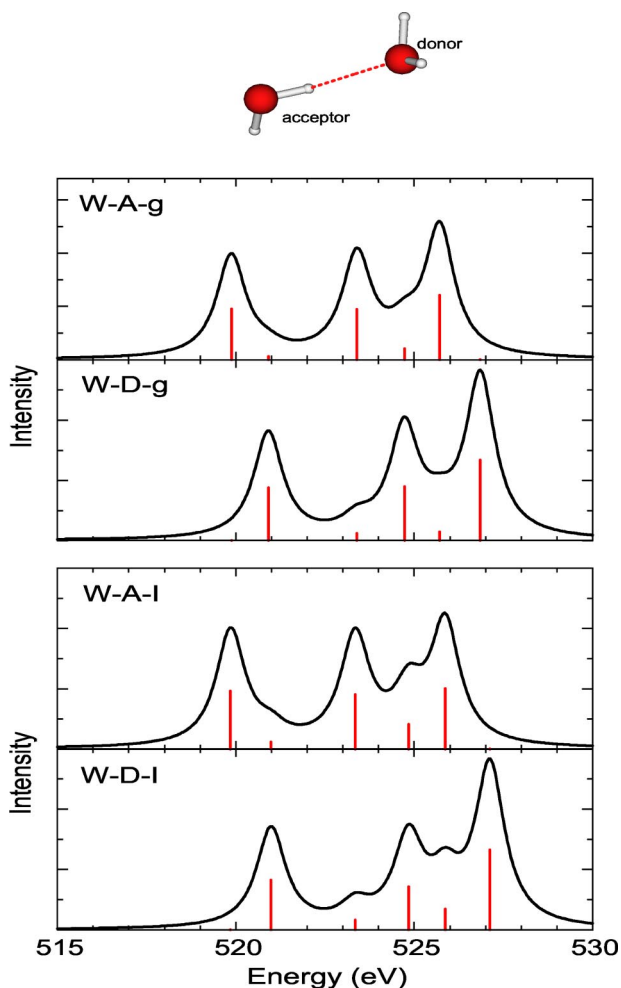


FIG. 6. X-ray emission spectra of water dimers in gas phase (*g*) and ice phase (*I*) with O-O distance 2.98 and 2.75 Å, respectively. Characters *W*, *A*, and *D* refer to the water molecule, hydrogen acceptor, and hydrogen donor, respectively. Vertical bars represent spectra without broadening.

What is also clear is that the observed strong orbital mixing in the x-ray emission spectra of liquid water cannot be explained by the gas phase or icelike water dimer calculations presented in Fig. 6. It is noticeable that the gas phase dimer used here possesses an optimized structure in the gas phase which can never really exist in either ice or liquid water. Therefore, it would be more relevant to calculate the spectra of a dimer that is generated from the liquid or ice. We have extracted out four possible dimer structures from the four hydrogen bonding structure *W-DDAA* described in the section above. The calculated spectra for these four dimers, shown in Fig. 7, are significantly different from those for the gas phase dimer. Orbital mixing can be found for all the cases. The relative spectral shifting follows the push-pull scheme discussed above, which is a net result of the static electric interaction. Depending on the mutual positioning of water molecules, orbital mixing can involve different orbitals. For instance, for oxygen donors, as in the cases *W-D1* and *W-D2*, the outermost orbital $1b_1$ of the “center” molecule strongly interacts with the $3a_1$ orbital of another water molecule, resulting in a reduction of the intensity of $1b_1$. In

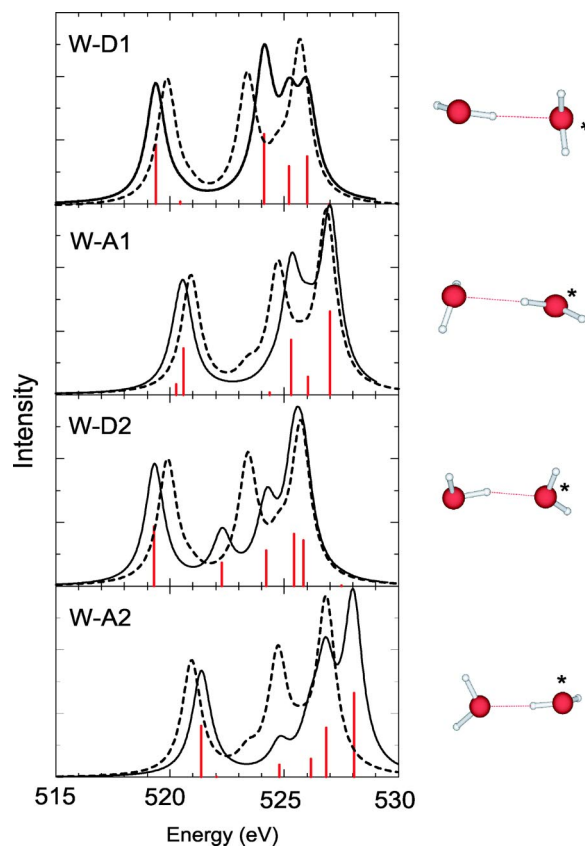


FIG. 7. X-ray emission spectra of water dimers generated from the structure *W-DDAA*. The excited oxygen is marked with an asterisk. The corresponding spectra for gas phase dimer are shown for comparison (dotted lines). Vertical bars represent spectra without broadening.

contrast, the $1b_1$ orbital of acceptors *W-A1* and *W-A2* is hardly involved in the interaction, instead the $3a_1$ orbital is strongly affected.

A comparison between the results shown in Figs. 6 and 7 indicates that the conclusion about the character of hydrogen bonding drawn from the analysis of gas phase dimer is irrelevant concerning the actual hydrogen bonding situations in liquid water. The mutual spatial arrangement of two water molecules in the liquid phase is enforced by the presence of other water molecules connected in a large hydrogen bonding network. This can result in various possible dimer configurations that are different from the gas phase. The electronic structure of the water molecule in the liquid is very sensitive to the positions of its neighbors. Therefore, the reliability of using interaction potentials generated from the gas phase dimer in the molecular dynamics simulation is questionable.

C. Water trimers

It is possible to construct six water trimers from the *W-DDAA* structure. The calculated x-ray emission spectra of those six trimers are given in Fig. 8. In this case, the center molecule is interacting with two others. It can be seen that the relative spectral shifting is dependent on the fine balance

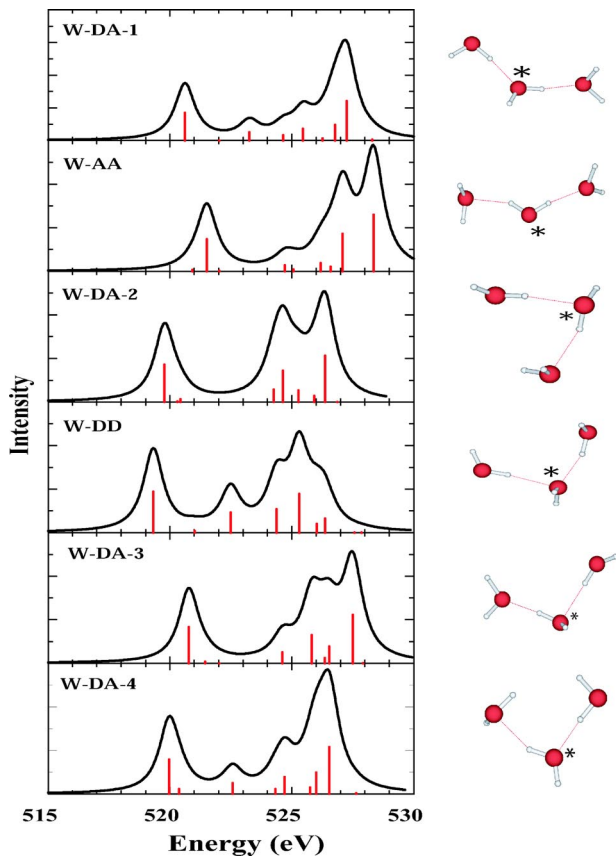


FIG. 8. X-ray emission spectra of water trimers generated from the *W-DDAA* structure. The excited oxygen is marked with an asterisk. Vertical bars represent spectra without broadening.

between the forces provided by water molecule on the donor and acceptor sides. The push-pull behavior is best illustrated by the relative spectral shifting of the *W-AA* and *W-DD* structures. The calculated spectra again indicate that the orbital mixing among water molecules is strongly dependent on their local arrangement.

We have seen that the experimental spectrum *D* in Fig. 3 is very different from the other two resonant spectra *P* and *S*. A new local structure that differs from the broken three hydrogen bonding structure *D-ASYM* is responsible for such a difference. The XAS simulations show that at this energy position, the most possible candidate would be a *W-DA* structure.¹³ Spectra generated from four *W-DA* structures show indeed an increase of intensity at the $3a_1$ region in comparison with the spectrum of *D-ASYM*. However, only *W-DA-2* and *W-DA-3* provide a broad spectral feature at the $3a_1$ region. Between these two, it seems that the spectrum of *W-DA-3* is in most close agreement with the experimental spectrum *D*.

D. Water tetramers

The strong electron sharing among water molecules can be further demonstrated by the calculated x-ray emission spectra of four tetramers generated from the *W-DDAA* structure, see Fig. 9. The spectral shifting can be understood by the push-pull behavior of donors and acceptors.

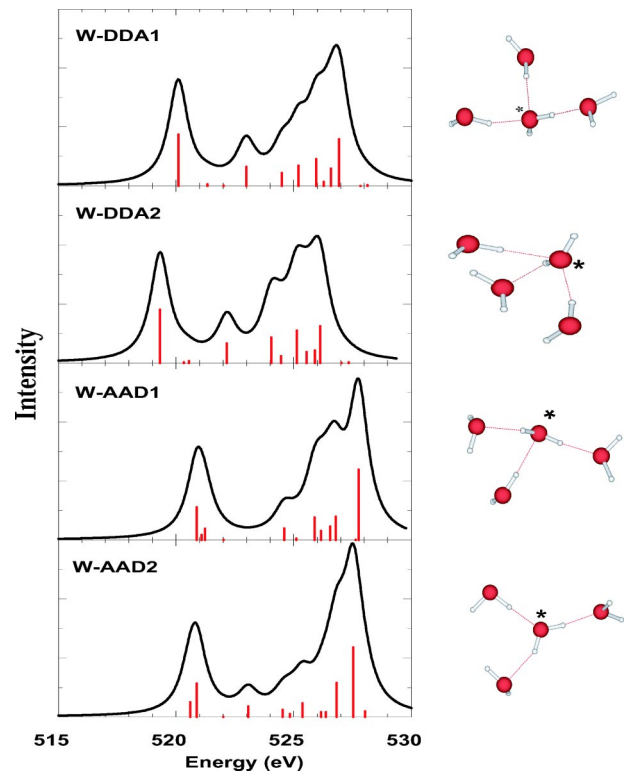


FIG. 9. X-ray emission spectra of water tetramers generated from the *W-DDAA* structure. The excited oxygen is marked with an asterisk. Vertical bars represent spectra without broadening.

The two *W-DDA* structures have the same donors, but different acceptor. It is noticed that for both structures, the $3a_1$ and the $1b_1$ orbitals of the center water molecule strongly interact with the surroundings. The spectral profile at the $3a_1$ and the $1b_1$ region is sensitive to the location of the acceptor, the outermost band generated from the *W-DDA2* structure is much broader than that from the *W-DDA1* structure. However, it should be noted that x-ray absorption of the *W-DDA* structures in the liquid water are always inside the continuum.¹³ Therefore, the *W-DDA* structures cannot be separated by the XES.

The *D-ASYM* structure identified by both XAS (Ref. 13) and XES (Ref. 2) is a *W-AAD* type of structure. For such a structure, the orbital mixing involves mainly the $1b_2$ and $3a_1$ orbitals, while the outermost lone pair orbital $1b_1$ is hardly affected. The spectral shape depends strongly on the position of the donor. The *W-AAD2* structure produces a spectrum that is closer to that of the big *D-ASYM* cluster. It should be mentioned that although the mutual positioning of acceptors and donor in the real *W-AAD* structures of liquid water can be quite different from the ones presented here, the overall picture of orbital interactions is expected to be the same.

VI. SUMMARY

We have demonstrated that x-ray emission spectroscopy is a powerful tool for studying the electronic and local geometrical structures of liquid water. We have interpreted the

strong electron sharing observed in the x-ray emission spectra of liquid water as a sign of covalency of hydrogen bonding. Calculations clearly show that the information about intermolecular interaction in the gas phase water dimer is irrelevant to the case of liquid water. The electronic structure of the water molecule is sensitive to the local arrangement of the hydrogen bondings. In all cases, the $3a_1$ orbital of the water molecule is affected the most. The outermost orbital $1b_1$ interacts with others only when strong donors are present. The x-ray emission of water in both gas and liquid phases is found to be dependent on the excitation energy. In the case of gas phase, such an excitation energy dependence can be understood in terms of the polarization or angular dependence of the resonant inelastic x-ray scattering processes, for which a simple analytical expression is used. On the other hand, the excitation energy dependence of the x-ray emission spectra of liquid water is found to be mostly related

to the variations of local hydrogen bonding structures. By selective excitations, we have been able to identify two local hydrogen bonding structures, one with two acceptors and one donor, another with one acceptor and one donor. It has been shown that the major spectral features of liquid water can be well described by the simulations of local hydrogen bonding structures within the first solvation shell.

ACKNOWLEDGMENTS

This work was supported by the Swedish Research Council (VR), the Göran Gustafsson Foundation for Research in Natural Science and Medicine, and the National Supercomputer Center (NSC) in Linköping, Sweden. The experimental work at ALS, Lawrence Berkeley National Laboratory was supported by the U.S. Department of Energy, under Contract No. DE-AC03-76SF00098.

*Email address: luo@theochem.kth.se

†Email address: jguo@lbl.gov

¹J. Nordgren, L.O. Werme, H. Ågren, C. Nordling, and K. Siegbahn, *J. Phys. B* **8**, L18 (1975).

²J.-H. Guo, Y. Luo, A. Augustsson, J.-E. Rubensson, C. S  the, H. Ågren, H. Siegbahn, and J. Nordgren, *Phys. Rev. Lett.* **89**, 1374021 (2002).

³G. Patey and G. Torrie, *Chem. Scr.* **29A**, 39 (1989).

⁴S. Knuts and H. Ågren, *Phys. Scr.* **T41**, 95 (1992).

⁵T. Privalov, F. Gel'mukhanov, and H. Ågren, *Phys. Rev. B* **64**, 165115 (2001).

⁶S. Woutersen, U. Emmerichs, and H. Bakker, *Science* **278**, 658 (1997).

⁷R. Laenen, C. Rauscher, and A. Lauberau, *Phys. Rev. Lett.* **80**, 2622 (1998).

⁸F.H. Stillinger, *Science* **209**, 451 (1980).

⁹A.K. Soper, *J. Chem. Phys.* **101**, 6888 (1994).

¹⁰R.A. Kuharski and P.J. Rossky, *J. Chem. Phys.* **82**, 5164 (1985).

¹¹A. Luzar and O. Chandler, *Phys. Rev. Lett.* **76**, 928 (1996).

¹²J.R. Errington and P.G. Debenedetti, *Nature (London)* **409**, 318 (2001).

¹³S. Myeneni, Y. Luo, L.  . N  slund, M. Cavalleri, L. Ojam  e, H. Ogasawara, A. Pelmenchikov, Ph. Wernet, P. V  terlein, C. Heske, Z. Hussain, L.G.M. Pettersson, and A. Nilsson, *J. Phys.: Condens. Matter* **14**, L213 (2002).

¹⁴A.J. Sadlej, *Theor. Chim. Acta* **79**, 123 (1991).

¹⁵T. Helgaker *et al.*, DALTON, *An ab initio electronic structure program*, Release 1.0, 1997. See <http://www.kjemi.uio/software/dalton/dalton.html>

¹⁶L. Ojam  e, I. Shavitt, and S.J. Singer, *J. Chem. Phys.* **109**, 5547

(1998).

¹⁷Y. Luo, H. Ågren, and F.Kh. Gel'mukhanov, *J. Phys. B* **27**, 4169 (1994).

¹⁸Y. Luo, H. Ågren, and F.Kh. Gel'mukhanov, *Phys. Rev. A* **53**, 1340 (1996).

¹⁹T. Warwick, P. Heimann, D. Mossessian, W. McKinney, and H. Padmore, *Rev. Sci. Instrum.* **66**, 2037 (1995).

²⁰J. Nordgren, G. Bray, S. Cramm, R. Nyholm, J.E. Rubensson, and N. Wassdahl, *Rev. Sci. Instrum.* **60**, 1690 (1989).

²¹H. Ågren, S. Svensson, and U.I. Wahlgren, *Chem. Phys. Lett.* **35**, 336 (1975).

²²H. Ågren and J. Nordgren, *Theor. Chim. Acta* **58**, 111 (1981).

²³J.-E. Rubensson, L. Petersson, N. Wassdahl, M. B  ckstr  m, J. Nordgren, O.M. Kvalheim, and R. Manne, *J. Chem. Phys.* **82**, 4486 (1985).

²⁴A. Cesar, H. Ågren, and V. Carravetta, *Phys. Rev. A* **40**, 1 (1989).

²⁵N. M  rtensson, P.-  . Malmqvist, S. Svensson, E. Basilier, J.J. Pireaux, U. Gelius, and K. Siegbahn, *Nouv. J. Chim.* **1**, 191 (1977).

²⁶A.V. Okotrub, V.D. Yumatov, and L.N. Mazlalov, *Proc. USSR Acad. Sci.* **275**, 1456 (1984).

²⁷L. Pauling, *The Nature of the Chemical Bond* (Cornell University Press, Ithaca, NY, 1960), p. 452.

²⁸E.D. Isaacs, A. Shukla, P.M. Platzman, D.R. Hamann, B. Barbiellini, and C.A. Tulk, *Phys. Rev. Lett.* **82**, 600 (1999).

²⁹T.K. Ghanty, V.N. Staroverov, P.R. Koren, and E.R. Davidson, *J. Am. Chem. Soc.* **122**, 1210 (2000).

³⁰B. Barbiellini and A. Shukla, *Phys. Rev. B* **66**, 235101 (2002).

³¹W. Klopper, J.G.C.M. van Duijneveldt-van de Rijdt, and F.B. van Duijneveldt, *Phys. Chem. Chem. Phys.* **2**, 2227 (2000).